

# Modified Capacitor-Assisted Z-Source Inverter Topology with Enhanced Boost Ability

Anh-Vu Ho<sup>\*</sup> and Tae-Won Chun<sup>†</sup>

<sup>\*</sup>School of Engineering, Eastern International University, Vietnam

<sup>†</sup>Department of Electrical Engineering, University of Ulsan, Ulsan, Korea

## Abstract

This paper presents a novel topology named a modified capacitor-assisted Z-source inverter (MCA-ZSI) based on the traditional ZSI. The impedance network of the proposed MCA-ZSI consists of two symmetrical cells coupled with two capacitors with an X-shape structure, and each cell has two inductors, two capacitors, and one diode. Compared with other topologies based on switched ZSI with the same number of components used at impedance network, the proposed topology provides higher boost ability, lower voltage stress across inverter switching devices, and lower capacitor voltage stress. The improved performances of the proposed topology are demonstrated in the simulation and experimental results.

**Key words:** Boost ability, Impedance network, Inverter, Switched-capacitor, Z-source inverter

## I. INTRODUCTION

A voltage source inverter (VSI) has been widely adopted in various industrial applications. However, it can only operate in the buck mode because its peak ac output voltage is always lower than the dc source voltage. To obtain a high ac output voltage, an extra dc boost converter can be connected at the rear-end VSI, which eventually increases the cost and size of the power converter. A dead-time that can prevent an arm short of the inverter leg may distort the ac output voltage waveform.

The power converter used to solve the aforementioned problems of the conventional VSI is the Z-source inverter (ZSI) [1]. The ZSI can operate in the buck-boost mode with a single power converter by regulating the shoot-through state, in which the upper and lower switches of the same inverter leg are turned on concurrently to boost the dc-link voltage of the inverter. Moreover, ZSI can eliminate the need for a dead time of the inverter. Owing to its unique features, it has been utilized at the uninterruptible power supply, grid-connected photovoltaic generation systems, wind power applications, and electric vehicle tractions [2]-[6]. However, because the

actual boost gain of the traditional ZSI is limited, it cannot be efficiently applied to further applications, which require a power converter with strong boost capability.

Recently, several ZSI-based topologies that strengthen the boost capability have been reported. To obtain a high boost factor with low shoot-through duty ratio, topologies with switched-inductor (SL) or/and switched-capacitor (SC) impedance networks based on the ZSI structure [7], [8] or quasi-ZSI structure [9]-[11] are introduced. In [12], the hybrid SL impedance source converter is proposed, to independently regulate ac and dc voltages for supplying both voltages to the ac and dc loads, respectively.

To raise the boost factor, the topologies that connect more cells in series at the impedance network are proposed in [13]-[16]. However, additional inductors, capacitors, and/or diodes in the impedance network are needed to further raise a dc-link voltage, which increase the cost and volume of the power converter. The coupled transformer-based or inductor-based ZSI configurations as the alternate approaches offer a high conversion gain by adjusting a turns-ratio of the coupled transformer or inductor [16]-[18]. In [19], the concept of switched boost inverter is extended to the transformer-based switched boost inverters to achieve a high boost factor with a low turn ratio of the transformer.

In this study, a novel topology based on the capacitor-assisted ZSI, which is called the modified capacitor-assisted ZSI (MCA-ZSI), is proposed to enhance

Manuscript received Apr. 13, 2017; accepted Jun. 22, 2017

Recommended for publication by Associate Editor Yun Zhang.

<sup>†</sup>Corresponding Author: twchun@mail.ulsan.ac.kr

Tel: +82-52-259-2188, Fax: +82-51-259-1686, University of Ulsan

<sup>\*</sup>School of Engineering, Eastern International University, Vietnam

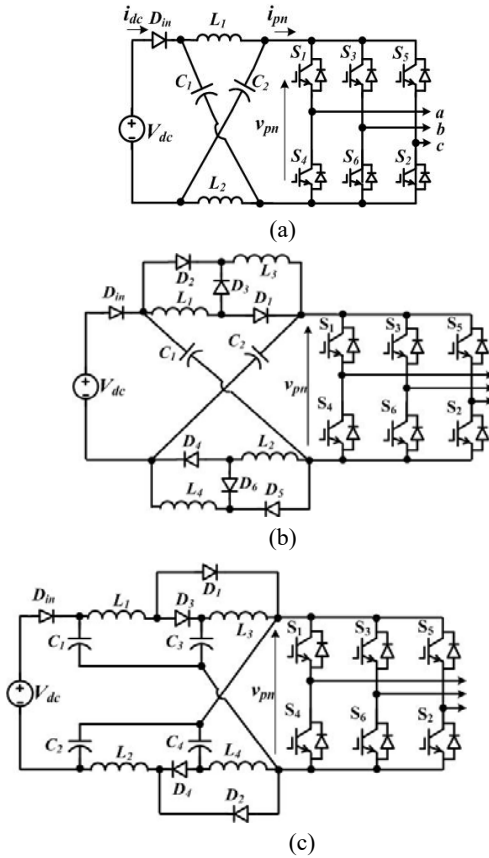


Fig. 1. Traditional ZSI and topologies based on switched ZSI: (a) traditional ZSI, (b) SL-ZSI, (c) EB-ZSI.

the boost capability. Comparisons with other topologies based on switched - inductor/capacitor ZSI recognize the improved performance of the proposed topology, as confirmed through the simulation and experimental results.

## II. REVIEW OF TRADITIONAL ZSI AND MODIFIED TOPOLOGIES BASED ON SWITCHED ZSI

A traditional ZSI and two topologies based on the switched-inductor/capacitor ZSI structure are shown in Fig. 1. Fig. 1(a) shows the traditional ZSI reported in [1]. Fig. 1(b) shows the SL-ZSI topology introduced in [7]. The impedance network in the SL-ZSI is constructed by replacing two inductors of the traditional Z-impedance network into two SL cells, where each SL cell is composed of two inductors and three diodes. Fig. 1(c) shows a novel topology called enhanced-boost ZSI (EB-ZSI) reported in [8], which is used to raise the boost factor. The impedance network in the EB-ZSI contains top and bottom cells coupled to the two X-shaped capacitor pairs, where each cell is composed of two inductors and two diodes.

The boost factor  $B$  is expressed as the ratio between the peak dc-link voltage  $\hat{v}_{pn}$  and the dc input voltage  $V_{dc}$ , and the boost factors of the traditional ZSI, SL-ZSI, and EB-ZSI

can be as follows:

$$B = \frac{\hat{v}_{pn}}{V_{dc}} = \frac{1}{1 - 2(T_0/T)} = \frac{1}{1 - 2D} \quad \text{for traditional ZSI} \quad (1)$$

$$B = \frac{1+D}{1-3D} \quad \text{for SL-ZSI} \quad (2)$$

$$B = \frac{1}{1-4D+2D^2} \quad \text{for EB-ZSI}, \quad (3)$$

where  $T_0$  is the shoot-through time during one switching interval  $T$  and  $D = T_0/T$  depicts the shoot-through duty ratio.

## III. PROPOSED MODIFIED CAPACITOR-ASSISTED ZSI

The operating principles and modulation techniques for the proposed MCA-ZSI are described as follows.

### A. Operating PRINCIPLES of Proposed MCA-ZSI

Fig. 2 shows the structure of the proposed MCA-ZSI, an impedance network that has symmetrical top and bottom cells coupled with two split capacitors ( $C_1$  and  $C_2$ ) with an X-shape structure. Moreover, the top and bottom cells have four inductors ( $L_1, L_2, L_3$ , and  $L_4$ ), four capacitors ( $C_3, C_4, C_5$ , and  $C_6$ ), and two diodes ( $D_2$  and  $D_3$ ). The operation states of MCA-ZSI are identical with those of the traditional ZSI, which are classified as the non-shoot-through state and shoot-through state.

Fig. 3 shows the equivalent circuits of the proposed MCA-ZSI in non-shoot-through and shoot-through states. The two X-shaped split capacitors and two cells in the impedance network are symmetrical due to the symmetrical structure of the proposed impedance network. When the four capacitors ( $C_3, C_4, C_5$ , and  $C_6$ ) and the four inductors ( $L_1, L_2, L_3$ , and  $L_4$ ) in the top and bottom cells and two split capacitors ( $C_1$  and  $C_2$ ) have the same capacitance and inductance, we have  $V_{C3} = V_{C4} = V_{C5} = V_{C6}$ ,  $V_{L1} = V_{L2} = V_{L3} = V_{L4}$ , and  $V_{C1} = V_{C2}$ .

In the non-shoot-through state, the MCA-ZSI operates in the same manner as the traditional inverter. During this state, three diodes are forward biased, and the four inductors and the dc input source supply the energies to the six capacitors. The dc-link voltage feeding to the external ac load can be obtained from the summation of three capacitor voltages. The two inductor voltages and one capacitor current at the top cell, X-shaped capacitor current, and dc-link voltage can be expressed as

$$V_{L1} = -V_{C3} = V_{C4} - V_{C2} + V_{dc} \quad (4)$$

$$V_{L2} = -V_{C4} = V_{C3} - V_{C2} + V_{dc} \quad (5)$$

$$i_{C1} = -i_{L1} + i_{C3} + i_{dc} \quad (6)$$

$$i_{C3} = i_{L1} - i_{L2} - i_{C4}, \quad i_{C4} = i_{L2} - i_{C2} - i_i \quad (7)$$

$$\hat{v}_{pn} = V_{C1} + V_{C3} + V_{C4} \quad (8)$$

In the shoot-through state, the dc-link terminal is shorted by turning on the upper and lower switching devices of any

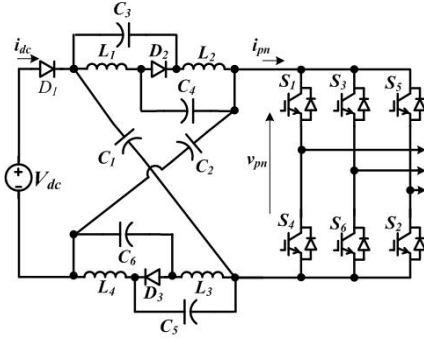


Fig. 2. Proposed MCA-ZSI.

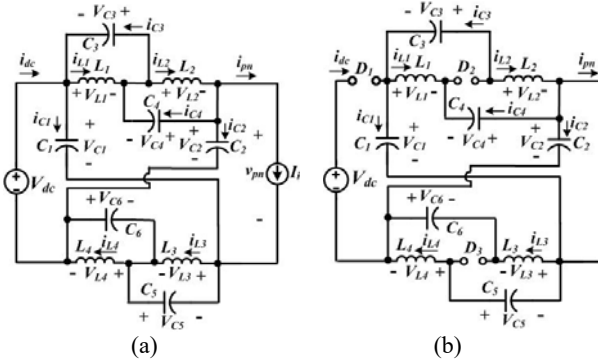


Fig. 3. Equivalent circuits of proposed MCA-ZSI: (a) in non-shoot-through state, (b) in shoot-through state.

phase leg of the inverter. During the shoot-through state, three diodes  $D_1$ ,  $D_2$ , and  $D_3$  are reverse biased and four inductors  $L_1$ ,  $L_2$ ,  $L_3$ , and  $L_4$  are charged from the six capacitors. The two inductor voltages, one capacitor current at the top cell, and one X-shaped capacitor current are written as

$$V_{L1} = V_{C1} + V_{C4} \quad (9)$$

$$V_{L2} = V_{C1} + V_{C3} \quad (10)$$

$$i_{C1} = i_{L1} - i_{C3} = i_{L1} + i_{L2} \quad (11)$$

$$i_{C3} = -i_{L2}, \quad i_{C4} = -i_{L1}. \quad (12)$$

Applying the principle that the average of the inductor voltage over one switching cycle is zero to two inductors  $L_1$  and  $L_2$  from (4), (5), (9), and (10) and using  $V_{C1} = V_{C2}$  and  $V_{C3} = V_{C4} = V_{C5} = V_{C6}$  obtained from the symmetry impedance network structure, three capacitor voltages  $V_{C1}$ ,  $V_{C3}$ , and  $V_{C4}$  at the top cell can be expressed as a function of shoot-through duty ratio, respectively.

$$V_{C1} = \frac{(1-2D)(1-D)}{1-5D+4D^2} V_{dc} \quad (13)$$

$$V_{C3} = V_{C4} = \frac{D(1-D)}{1-5D+4D^2} V_{dc} \quad (14)$$

Substituting (13) and (14) into (8), the boost factor of the proposed MCA-ZSI can be derived as

$$B = \frac{\hat{v}_{pn}}{V_{dc}} = \frac{1-D}{1-5D+4D^2}. \quad (15)$$

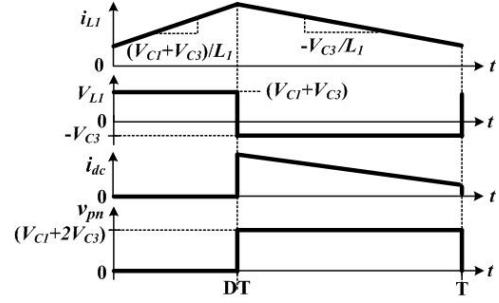


Fig. 4. Waveforms of proposed MCA-ZSI.

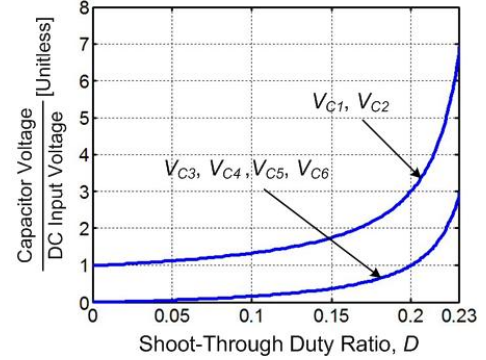


Fig. 5. Capacitor voltage stress ratio of proposed MCA-ZSI with various shoot-through duty ratios.

The ac output gain  $G$  is defined as the conversion gain of the peak of the ac output voltage  $\hat{v}_{ac}$  to dc input voltage  $V_{dc}$ , and it can be expressed as the modulation index  $M$  and boost factor  $B$ .

$$G = M \cdot B = \frac{\hat{V}_{ac}}{V_{dc}/2} \quad (16)$$

Fig. 4 shows the waveforms of the inductor current and voltage, dc input current, and dc-link voltage. The inductor current increases during the shoot-through state and decreases during the shoot-through state. The dc input current is discontinuous and can be obtained from (6) in the non-shoot-through state. The dc-link voltage can be boosted by adding  $V_{C1}$  and twice of  $V_{C3}$  in the non-shoot-through state.

Fig. 5 shows the ratio of the voltage stress of six capacitors utilized at the impedance network of the proposed MCA-ZSI to the dc input voltage with a variation of the shoot-through duty ratio. It can be seen that the voltage stress of four capacitors ( $C_3$ ,  $C_4$ ,  $C_5$ , and  $C_6$ ) is approximately 2.5 times lower than the voltage stress of two capacitors ( $C_1$  and  $C_2$ ).

Applying the principle that the average of the capacitor current  $i_{C1}$  over one switching cycle is zero to capacitor  $C_1$  from (6) and (11) and using  $i_{L1} = i_{L2} = i_{L3} = i_{L4} = i_L$  obtained from the symmetry impedance network structure, we can derive the average of inductor current as

$$\bar{i}_L = \frac{1-D}{4D} (i_{dc} - I_i). \quad (17)$$

Assuming that all components of the MCA-ZSI are ideal, as the dc input power is identical to the dc-link power such as

$V_{dc} \cdot i_{dc} = \hat{v}_{pn} \cdot I_i$ , the dc-link current in the non-shoot-through state is expressed as the dc input current.

$$I_i = \frac{1-5D+4D^2}{1-D} i_{dc}. \quad (18)$$

Substituting (18) into (17), the current stress of four inductors can be expressed as the shoot-through duty ratio and dc input current.

$$\bar{i}_L = (1-D)i_{dc} \quad (19)$$

### B. Modulation Technique

A modulation scheme for the proposed topology focuses on efficiently embedding the shoot-through state within a zero state to enhance the boost capability while the active state remains fixed. The ac output gain is dependent on the combination of  $M$  and  $B$  in (16). One switching period is shared by the non-shoot-through state and the shoot-through state. Thus, the ac output gain influences the modulation techniques due to the trade-off between  $M$  and  $D$ . Among the three carrier-based modulation techniques, namely, simple control, constant boost control, and maximum boost control techniques [20], the constant boost control technique reported in [21] is utilized at the proposed topology to remove the low-frequency voltage and current ripples and obtain a high-voltage boost ability with low possible value of  $D$ .

The maximum modulation index with a given  $D$  can be drawn as  $M = (2/\sqrt{3})(1-D)$  by using the constant boost control method. As a result, a high ac output voltage with a given low  $D$  can be produced.

## IV. COMPARISON OF PROPOSED MCA-ZSI WITH OTHER TOPOLOGIES

This section describes a comparison analysis of performances among the proposed MCA-ZSI, traditional ZSI, SL-ZSI, and EB-ZSI. These topologies are compared on the basis of their boost factor, voltage stress of inverter switching devices, capacitor voltage stress, and number of components utilized at the impedance network.

Fig. 6 shows the boost factors of four topologies according to a variation of shoot-through duty ratio. Among the four topologies, the proposed MCA-ZSI has the highest boost factor in the total range of the shoot-through duty ratio. Therefore, the proposed MCA-ZSI can produce a high ac output voltage with a low shoot-through duty ratio. Fig. 7 presents the ratio of the voltage stress across inverter switches to the minimum dc input voltage with a variation of ac voltage gain  $G$  for the four topologies. It can be noted that the proposed MCA-ZSI has the lowest voltage stress across inverter switching devices among the four topologies, which can save the cost of the power converter. Fig. 8 shows the ratio of the capacitor voltage stress to the dc input voltage with various boost factors  $B$  for the four topologies. The

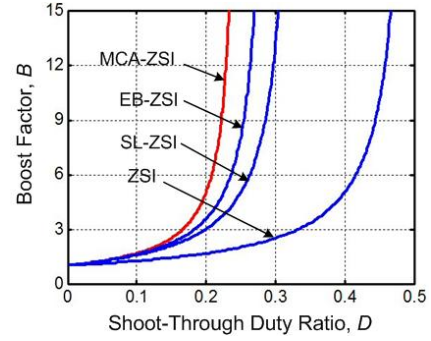


Fig. 6. Boost factors of four topologies.

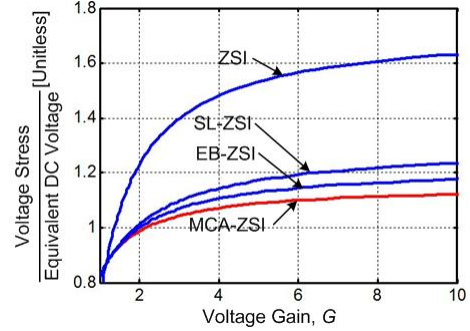


Fig. 7. Voltage stress ratio of four topologies.

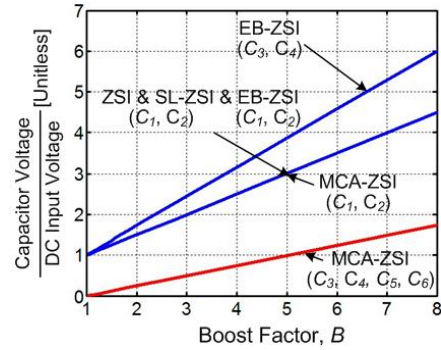


Fig. 8. Capacitor voltage stress ratio of four topologies.

voltage stress of the two capacitors of the MCA-ZSI ( $C_1$  and  $C_2$ ) is the same as the voltage stress of the two capacitors of the EB-ZSI, SL-ZSI, and traditional ZSI. The voltage stress of the four capacitors of the MCA-ZSI ( $C_3$ ,  $C_4$ ,  $C_5$ , and  $C_6$ ) is much lower than the capacitor voltage stress of the other topologies, and the two capacitors of the EB-ZSI ( $C_3$  and  $C_4$ ) have the highest capacitor voltage stress.

Table I reports the comparison of the number of passive components and diodes used at the impedance network in the proposed MCA-ZSI, EB-ZSI, SL-ZSI, and traditional ZSI. The number of inductors required at the MCA-ZSI, EB-ZSI, and SL-ZSI is identical. Although the proposed MCA-ZSI needs two or four capacitors more than the other three topologies, four to six capacitors have low capacitor voltage stress. Additionally, two or four diodes can be saved. In conclusion, the total number of components utilized at the impedance network of the MCA-ZSI is the same as that of the other two topologies except the traditional ZSI, whereas

TABLE I  
NUMBER OF COMPONENTS AT IMPEDANCE NETWORK

Topologies	Inductors	Capacitors	Diodes
MCA-ZSI	4	6	3
EB-ZSI	4	4	5
SL-ZSI	4	2	7
ZSI	2	2	3

the voltage stress of the four capacitors of the MCA-ZSI is approximately 2.5 times lower than that of the other topologies.

## V. SIMULATION AND EXPERIMENTAL RESULTS

In order to demonstrate the enhanced boost ability of the proposed topology, both the simulation and experiments are performed with the following circuit parameters:

- Impedance network:  $L_1 = L_2 = L_3 = L_4 = 1$  mH;  
 $C_1 = C_2 = C_3 = C_4 = C_5 = C_6 = 1000$   $\mu$ F;
- Three-phase LC output filter:  $L_f = 0.6$  mH,  $C_f = 100$   $\mu$ F;
- Three-phase resistive-inductance load:  $R = 60$   $\Omega$ ,  
 $L = 1.2$  mH;
- Switching frequency = 5 kHz.

### A. Simulation Results

The simulation studies are carried out on the open loop control of the proposed topology in PSIM program, neglecting the equivalent series resistances (ESRs) in the inductors and capacitors and the forward voltage drop of switching devices and diodes. Fig. 9 shows the simulation results when  $M = 0.91$ ,  $D = 0.214$ , and  $V_{dc} = 50$  V. The capacitor voltages  $V_{C1}$  and  $V_{C3}$  are put up to 200 V and 75 V from the dc input voltage of 50 V, respectively, and the peak of dc-link voltage is 350 V. The ac output voltage with 190 Vrms can be produced. From Fig. 9(b), during shoot-through state, the dc input current is zero, and the inductor current increases while the dc-link voltage is zero. The dc-link voltage has a peak voltage and the inductor current decreases in non-shoot-through state. The average inductor current is approximately 15 A, which can be calculated by multiplying the average dc input current at non-shoot-through period (19 A) by the non-shoot-through duty ratio  $(1 - D) = 0.786$  from (19).

Fig. 10 shows the simulation waveforms when  $M = 0.93$ ,  $D = 0.195$  at the same dc input voltage as 50 V. The shoot-through duty ratio is reduced from 0.214 to 0.195. Thus, the capacitor voltages  $V_{C1}$  and  $V_{C3}$  decrease from 200 V and 75 V to 135 V and 45 V, respectively, where  $V_{C3}$  is slightly lower than the dc input voltage. The ac output voltage is shrunk to 128 Vrms in spite of increasing the modulation index  $M$  from 0.91 to 0.93, because the dc-link voltage decreases from 350 V to 225 V as  $D$  decreases from 0.21 to 0.195.

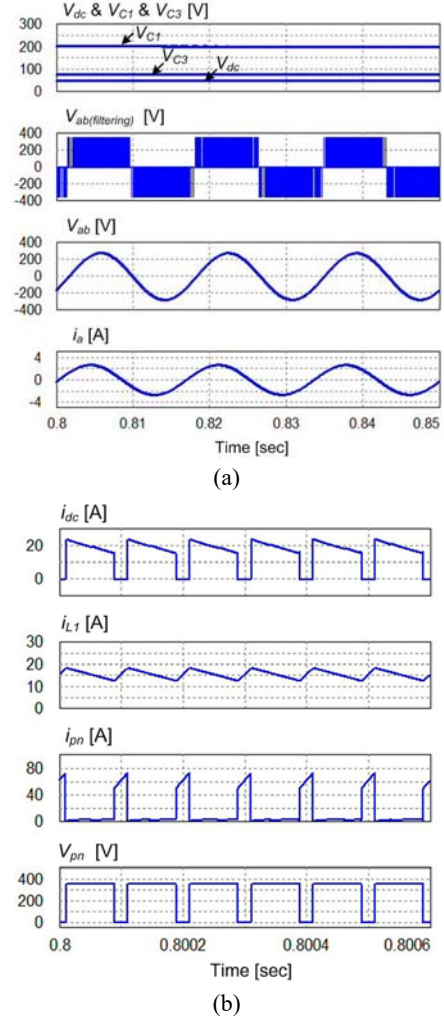


Fig. 9. Simulation waveforms of MCA-ZSI at  $M = 0.91$ ,  $D = 0.214$ : (a) capacitor and dc input voltages, ac output voltage and current (b) dc input and inductor currents, dc-link current and voltage.

To summarize the simulation results, Table II describes the values of capacitor voltages, dc-link voltage, ac output voltages, and inductor current at the two operating conditions.

### B. Experimental Results

In Fig. 11, the experimental system setup built in the laboratory is shown. It consists of three-phase inverter, impedance network, LC filter, RL load, and DSP control board. The 32-bit DSP TMS 320F28335 is utilized to generate the PWM signals including the shoot-through state.

Fig. 12 shows the experimental results of the identical operating conditions with the simulation results shown in Fig. 9. As shown in Fig. 12, the capacitor voltages  $V_{C1}$  and  $V_{C3}$  are raised to 195 V and 72 V, respectively. The dc-link voltage can be put up to 6.8 times from 50 V dc input voltage, and the RMS value of line-to-line voltage filtered by an LC filter is 185 V. The a-phase output current  $i_a$  has a nearly sinusoidal waveform with an RMS value of approximately 1.8 A. This value lags to the line-to-line voltage by more than  $30^\circ$ . Fig.



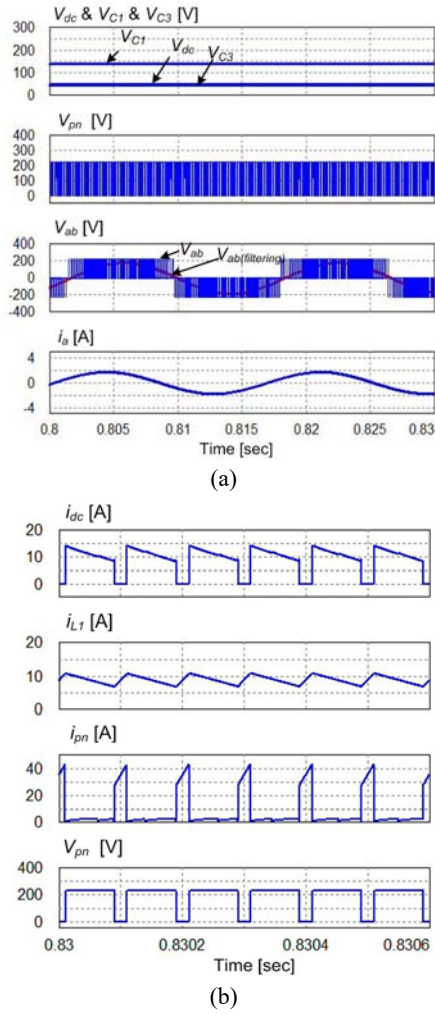


Fig. 10. Simulation waveforms of MCA-ZSI at  $M = 0.93$ ,  $D = 0.195$ : (a) capacitor and dc input voltages, ac output voltage and current (b) dc input and inductor currents, dc-link current and voltage.

TABLE II  
SUMMARY OF SIMULATION RESULTS

Operating Conditions	$V_{C1}$	$V_{C3}$	$\hat{v}_{pn}$	$V_{ab}$	$\bar{i}_L$
$M = 0.91$ $D = 0.214$	200 V	75 V	350 V	190 V	15 A
$M = 0.93$ $D = 0.195$	135 V	45 V	225 V	225 V	9 A

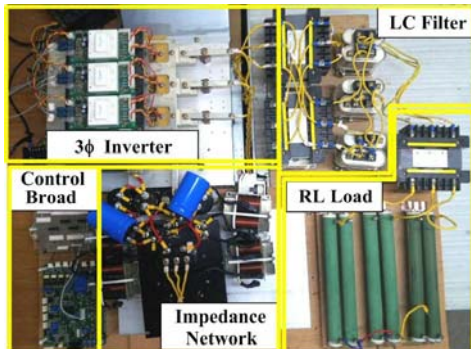


Fig. 11. Photograph of experimental system setup.

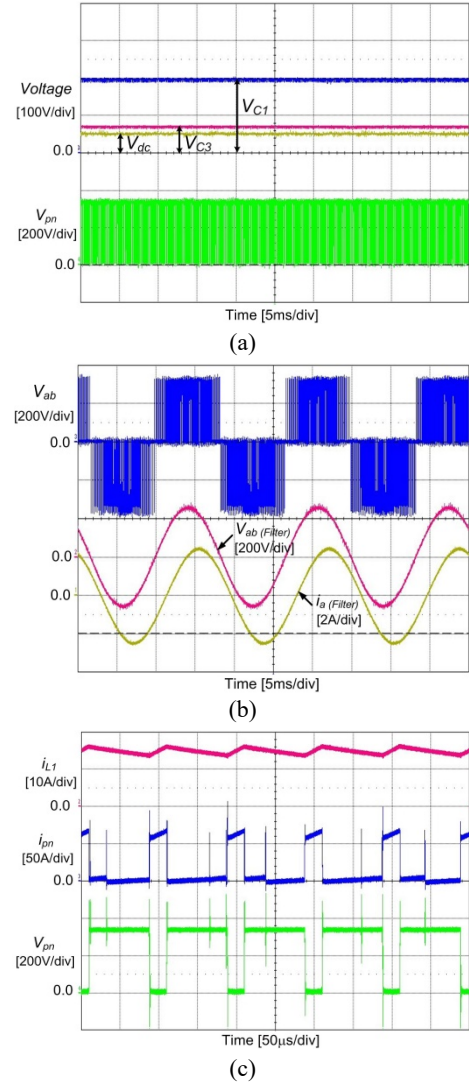


Fig. 12. Experimental results of MCA-ZSI at  $M = 0.91$ ,  $D = 0.214$ : (a) two capacitor voltages, dc input and dc-link voltages, (b) ac output voltage, filtered ac output voltage, and phase current, (c) inductor current, dc-link current, and voltage.

12(c) shows the experimental waveforms of inductor current, dc-link current, and dc-link voltage during three switching cycles.

Fig. 13 shows the experimental results of the identical operating conditions with the simulation results shown in Fig. 10. As shown in Fig. 13, the dc-link voltage can be put up approximately 4.25 times from 50 V dc input voltage, and the ac output voltage and current, inductor, and dc-link currents are decreased due to a low shoot-through duty ratio. Fig. 14 describes the efficiency of the proposed MCA-ZSI with a variation of output power at different shoot-through duty ratios. It can be noted that the proposed MCA-ZSI has more than 82% efficiency, and the efficiency at  $D = 0.15$  is higher than that at  $D = 0.2$ .

In comparison to simulation results, the capacitor, dc-link voltages, and ac output voltage of the experimental results are slightly lower, owing to ESRs in the inductances and

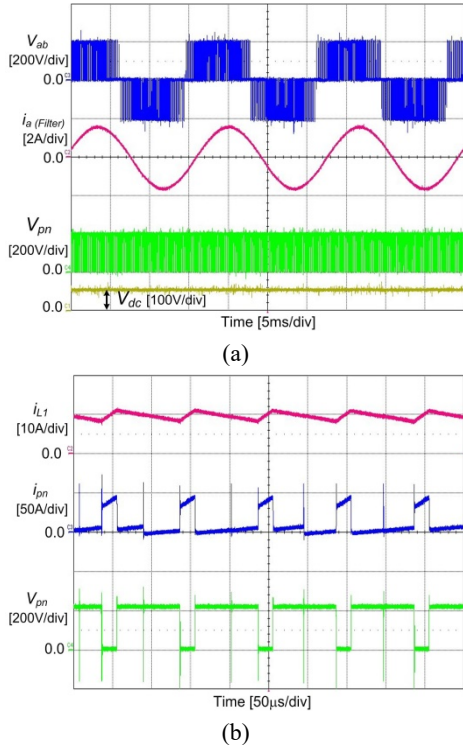


Fig. 13. Experimental results of MCA-ZSI at  $M = 0.93$ ,  $D = 0.195$ : (a) ac output voltage and current, dc-link and dc input voltages, (b) inductor current, dc-link current, and voltage.

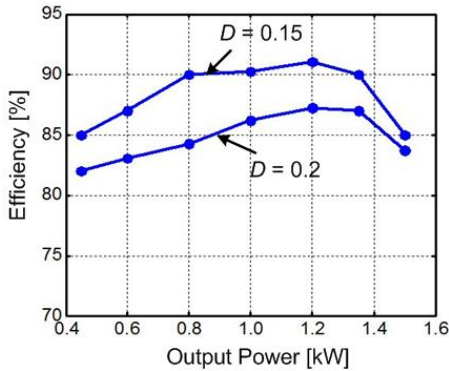


Fig. 14. Efficiency of MCA-ZSI with different shoot-through duty ratios.

capacitances and the forward voltage drop of diodes and switching devices. It can be noted that the experimental results are nearly consistent with the simulation results and theoretical analysis.

## VI. CONCLUSIONS

This paper proposed an MCA-ZSI topology used to improve the boost capability. Comparing the two different topologies based on switched ZSI, we find that the proposed MCA-ZSI topology has higher boost factor, lower voltage stress across switching devices, and much lower voltage stress of four capacitors, whereas the total number of components used at the impedance network is identical with

that of the other topologies. As validated by the experimental results, the dc-link voltage can be raised by approximately 6.8 times, and the ac output voltage with 185 Vrms can be generated from 50 V dc input voltage at a low shoot-through duty ratio of 0.214. The proposed MCA-ZSI has more than 82% efficiency. The proposed topology is suited to renewal generation systems with a low-voltage source.

## ACKNOWLEDGMENT

This work was supported by the 2016 Research Fund of University of Ulsan.

## REFERENCES

- [1] F. Z. Peng, "Z-source inverter," *IEEE Trans. Ind. Appl.*, Vol. 39, No. 2, pp. 504-510, Mar. 2003.
- [2] Z. Rymarski and K. Bernacki, "Influence of Z-source output impedance on dynamic properties of single-phase voltage source inverters for uninterrupted power supply," *IET Power Electron.*, Vol. 7, No. 8, pp. 1978-1988, 2014.
- [3] D. Vinnikov, A. Chub, E. Liivik, and I. Roasto, "High-performance quasi-Z-source series resonant DC-DC converter for photovoltaic module-level power electronics applications," *IEEE Trans. Power Electron.*, Vol. 32, No. 5, pp. 3634-3650, May, 2017.
- [4] Y. Liu, B. Ge, H. Abu-Rub, and F. Z. Peng, "An effective control method for three-phase quasi-Z-source cascaded multilevel inverter based grid-tie photovoltaic power system," *IEEE Trans. Ind. Electron.*, Vol. 61, No. 12, pp. 6794-6802, Dec. 2014.
- [5] C. L. Kala-Konga, M. N. Gitau, and R.C. Bansal, "Steady-state and small-signal models of a three-phase quasi-Z-source AC-DC converter for wind applications," *IET Renew. Power Gener.*, Vol. 10, No. 7, pp. 1033-1040, 2016.
- [6] H. Zhu, D. Yu, W. Zhu and Z. Zhou, "DC-link voltage regulation of bidirectional quasi-Z-source inverter for electric vehicle Applications," in *Proc. IEEE-VPPC*, pp. 1-5, 2016.
- [7] M. Zhu, K. Yu, and F. L. Luo, "Switched inductor Z-source inverter," *IEEE Trans. Power Electron.*, Vol. 25, No. 8, pp. 2150-2158, Aug. 2010.
- [8] H. Fathi and H. Madadi, "Enhanced-boost Z-source inverter with switched Z-impedance," *IEEE Trans. Ind. Electron.*, Vol. 63, No. 2, pp. 691-703, Feb. 2016.
- [9] M. K. Nguyen, Y. C. Lim, and G. B. Cho, "Switched-inductor quasi-Z-source inverter," *IEEE Trans. Power Electron.*, Vol. 26, No. 11, pp. 3183-3191, Nov. 2011.
- [10] K. Deng, J. Zheng, and J. Mei, "Novel switched-inductor quasi-Z-source inverter", *Journal of Power Electronics*, Vol. 14, No. 1, pp. 11-21, Jan. 2014.
- [11] M. K. Nguyen, Y. C. Lim, and J. H. Choi, "Two switched-inductor quasi-Z-source inverters," *IET Power Electron.*, Vol. 5, No. 7, pp. 1017-1025, Aug. 2012.
- [12] V. R. Vakacharla, M. Raghuram, and S. K. Singh, "Hybrid switched inductor impedance source converter – A decoupled approach," *IEEE Trans. Power Electron.*, Vol.

- 31, No. 11, pp. 7509-7521, Nov. 2016.
- [13] Y. P. Siwakoti, F. Z. Peng, F. Blaabjerg, P. C. Loh, and G. E. Town, "Impedance-source networks for electric power conversion part I: A topology review," *IEEE Trans. Power Electron.*, Vol. 30, No. 2, pp. 699-716, Feb. 2015.
  - [14] Q. N. Trinh and H. H. Lee, "A new Z-source inverter topology with high voltage boost ability," *Journal of Elect. Eng. & Technology*, Vol. 7, No. 5, pp. 714-723, 2012.
  - [15] D. Li, P. C. Loh, M. Zhu, F. Gao, and F. Blaabjerg, "Generalized multicell switched-inductor and switched-capacitor Z-source inverter," *IEEE Trans. Power Electron.*, Vol. 28, No. 2, pp. 837-848, Feb. 2013.
  - [16] W. Qian, F. Z. Peng, and H. Cha, "Trans-Z-source inverters," *IEEE Trans. Power Electron.*, Vol. 26, No. 12, pp. 3453-3463, Dec. 2011.
  - [17] S. D. Tavakoli, J. Khajesalehi, M. Hamzeh, and K. Sheshyekani, "Decentralised voltage balancing in bipolar dc microgrids equipped with trans-Z-source interlinking converter," *IET Renew. Power Gener.*, Vol. 10, No. 5, pp. 703-712, May 2016.
  - [18] S. Shubhra and S. Misha, "A coupled inductor based high boost inverter with sub-unity turns-ratio range," *IEEE Trans. Power Electron.*, Vol. 31, No. 11, pp. 7534-7543, Nov. 2016.
  - [19] M. K. Nguyen, Y. C. Lim, J. H. Choi, and Y. O. Choi, "Trans-switched boost inverters," *IET Power Electron.*, Vol. 9, No. 5, pp. 1065-1073, Apr. 2016.
  - [20] Y. P. Siwakoti, F. Z. Peng, F. Blaabjerg, P. C. Loh, G. E. Town, and S. Yang, "Impedance-source networks for electric power conversion part II: Review of control and modulation techniques," *IEEE Trans. Power Electron.*, Vol. 30, No. 4, pp. 1887-1906, Apr. 2015.
  - [21] M. Shen, J. Wang, A. Joseph, F. Z. Peng, L. M. Tolbert, and D. J. Adams, "Constant boost control of the Z-source inverter to minimize current ripple and voltage stress," *IEEE Trans. Ind. Appl.*, Vol. 42, No. 3, pp. 770-778, May/Jun. 2006.



**Anh-Vu Ho** was born in Vietnam in 1981. He received the B.S. and M.S. degrees in electrical engineering from the HoChiMinh City University of Technical Education, Vietnam, in 2005 and 2009, respectively. He received the Ph. D. degree in electrical engineering at Ulsan University, Korea in 2015. He is a lecturer with the School of Engineering, Eastern International University, Vietnam. His current research interests include power converters/inverters, power quality, and renewable energy systems.



**Tae-Won Chun** was born in Korea in 1959. He received his B.S. degree in electrical engineering from Pusan National University in 1981, and received the M.S. and Ph.D. degrees in electrical engineering from Seoul National University in 1983 and 1987, respectively. Since 1986, he has been a member of the faculty of the Department of Electrical Engineering, Ulsan University, where he is currently a full Professor. He was with the Department of Electrical and Computer Engineering, University of Tennessee, USA as a visiting scholar. From 2005 to 2006, he also served as a visiting scholar at the Department of Electrical and Computer Engineering, Virginia Polytechnic Institute and State University, USA. His current research interests are grid-connected inverter systems and ac motor control.